

# Tumor-suppressive functions of 15-Lipoxygenase-2 and RB1CC1 in prostate cancer

Mahipal V Suraneni<sup>1,†</sup>, John R Moore<sup>1</sup>, Dingxiao Zhang<sup>1</sup>, Mark Badeaux<sup>1</sup>, Marc D Macaluso<sup>1</sup>, John DiGiovanni<sup>2</sup>, Donna Kusewitt<sup>1</sup>, and Dean G Tang<sup>1,3,\*</sup>

<sup>1</sup>Department of Molecular Carcinogenesis; The University of Texas MD Anderson Cancer Center; Smithville, TX USA; <sup>2</sup>Division of Pharmacology and Toxicology; College of Pharmacy; The University of Texas at Austin; Austin, TX USA; <sup>3</sup>Cancer Stem Cell Institute; Research Center for Translational Medicine; Shanghai East Hospital; Tongji University School of Medicine; Shanghai, China

<sup>†</sup>Current affiliation: Flagship Biosciences; Boulder, CO USA

**Keywords:** 15-lipoxygenase-2, c-Myc, RB1CC1, prostate cancer, tumor suppression, senescence

15-Lipoxygenase-2 (15-LOX2) is a human-specific lipid-peroxidizing enzyme most prominently expressed in epithelial cells of normal human prostate but downregulated or completely lost in > 70% of prostate cancer (PCa) cases. Transgenic expression of 15-LOX2 in the mouse prostate surprisingly causes hyperplasia. Here we first provide evidence that 15-LOX2-induced prostatic hyperplasia does not progress to PCa even in p53<sup>+/-</sup> or p53<sup>-/-</sup> background. More important, by generating 15-LOX2; Hi-Myc double transgenic (dTg) mice, we show that 15-LOX2 expression inhibits Myc-induced PCa development, such that in the 3-month- and 6-month-old dTg mice, there is a significant reduction in prostate intra-neoplasia (PIN) and PCa prevalent in age-matched Hi-Myc prostates. The dTg prostates show increased cell senescence and expression of several senescence-associated molecules, including p27, phosphorylated Rb, and Rb1cc1. We further show that in HPCa, 15-LOX2 and c-Myc manifest reciprocal protein expression patterns. Moreover, RB1CC1 accumulates in senescing normal human prostate (NHP) cells, and in both NHP and RWPE-1 cells, the 15-LOX2 metabolic products 15(S)-HPETE and 15(S)-HETE induce RB1CC1. We finally show that unlike 15-LOX2, RB1CC1 is not lost but rather frequently overexpressed in PCa samples. RB1CC1 knockdown in PC3 cells enhances clonal growth in vitro and tumor growth in vivo. Together, our present studies provide evidence for tumor-suppressive functions for both 15-LOX2 and RB1CC1.

## Introduction

15-Lipoxygenase-2 (15-LOX2) is a lipid-peroxidizing enzyme that possesses several unique features compared with other lipoxygenase family members. Unlike widespread expression of 15-LOX1 and 12-LOX, 15-LOX2 is restricted to epithelial cells of a limited number of tissues including the prostate, skin, esophagus, and cornea.<sup>1,2</sup> Also unlike 15-LOX1 and 12-LOX, 15-LOX2 metabolizes membrane phospholipid arachidonic acid (AA) exclusively to generate 15(S)-HETE. 15-LOX2, a human-specific gene not expressed in rodents, shares only ~40% amino acid identity with 15-LOX1. However, it shares 78% sequence homology with mouse 8-LOX.<sup>3,4</sup> Although 8-LOX can be induced in mouse skin upon phorbol ester treatment, its expression is not observed in the mouse prostate.<sup>5</sup> Furthermore, in contrast to 5-LOX, 12-LOX, and 15-LOX1, which show pro-tumorigenic functions in prostate, 15-LOX2 seems to be anti-tumorigenic.<sup>6</sup>

Since 15-LOX2 is normally expressed in the luminal-layer prostate epithelial cells, our lab first focused on its biological functions in normal human prostate (NHP) epithelial cells. Our previous studies have demonstrated that: (1) 15-LOX2 functions

as a negative cell cycle regulator in NHP cells<sup>7</sup> and localizes in the cytoplasm as well as in the nucleus and cell–cell borders in vitro and in benign glands;<sup>8,9</sup> (2) 15-LOX2 has at least 6 splice variants, which are termed 15-LOXsv-a to 15-LOX2sv-f.<sup>7,9</sup> These splice variants have little to no AA-metabolizing activity and generally do not localize to the nucleus; (3) 15-LOX2 expression in NHP cells is positively regulated by Sp1 but negatively regulated by Sp3 and is not directly regulated by androgen/AR;<sup>10</sup> (4) 15-LOX2 expression in the human prostate correlates with age and in cultured primary NHP cells is cell-autonomously induced.<sup>11</sup> Primary NHP cells from normal prostates and cultured in serum/androgen-free, defined medium are CK5<sup>+</sup>CK18<sup>+</sup>CD44<sup>+</sup>α2β1<sup>+</sup>hTERT<sup>+</sup>p63<sup>+</sup>15LOX2<sup>-</sup>AR<sup>-</sup>PSA<sup>-</sup> intermediate progenitor cells that have a limited proliferative lifespan restricted by the senescence checkpoint.<sup>11–14</sup> 15-LOX2 appears to represent a regulator of NHP cell senescence,<sup>9,11,12,14</sup> as enforced expression of 15-LOX2 promotes senescence. 15-LOX2 expression is down-regulated or lost in the precursor lesion HGPIN (high-grade prostate intraepithelial neoplasia) as well as >70% prostate cancer (PCa).<sup>7,9,15,16</sup> In >20 immortalized prostate epithelial and PCa cell lines we have analyzed, 15-LOX2 expression is undetectable.<sup>7–9,12</sup>

\*Correspondence to: Dean G Tang; Email: dtang@mdanderson.org

Submitted: 02/25/2014; Revised: 03/30/2014; Accepted: 04/02/2014; Published Online: 04/14/2014  
<http://dx.doi.org/10.4161/cc.28757>

Restoration of 15-LOX2 expression in PCa cells inhibits proliferation, induces senescence-like phenotypes, and, importantly, abrogates tumor regeneration in xenograft models.<sup>7-9,11</sup>

The above-discussed studies on 15-LOX2 expression/functions in NHP and PCa cells imply a tumor-suppressive function for this molecule. To determine whether 15-LOX2 truly possesses (prostate) tumor-suppressive functions in vivo, we have recently generated prostate-specific transgenic (Tg) mice using the ARR2Pb promoter<sup>17</sup> to drive the expression of full-length (fl) 15-LOX2 or, for comparison, 15-LOX2 splice variant b (15LOX2-svb) that lacks enzymatic activity.<sup>18</sup> Three 15-LOX2 (fl2, fl15, fl26) and 3 15LOX2-svb (svb9, svb10, svb15) Tg lines were established that exhibited various levels of transgene expression.<sup>18</sup> Subsequent characterizations and functional studies in fl26 and svb9 lines revealed 2 surprising findings: macroscopically, the fl26, and, in particular, the svb9 Tg prostates, were larger than the age-matched wild-type (WT) prostates; and microscopically, the fl26 prostates, and, less obviously, svb9 prostates, showed hyperplasia, which did not progress to PIN (prostate intraepithelial neoplasia) or adenocarcinoma.<sup>18</sup> The seeming “contradiction” in the fl26 prostates with prominent hyperplasia but less enlargement of the organ (compared with the svb9 prostates) was explained by the early and more prominent induction of cell senescence, evidenced by both senescence-associated  $\beta$ -galactosidase (SA- $\beta$ gal) staining and increased molecular markers of senescence such as p27 and Rb1cc1,<sup>18</sup> an Rb1-inducible protein linked to inhibition of cell proliferation and induction of senescence.<sup>19-22</sup>

In the current study, we attempted to determine whether 15-LOX2 possesses in vivo anti-tumor properties by crossing 15-LOX2fl26 Tg animals with PCa-prone Hi-Myc mouse model.<sup>23</sup> We chose Hi-Myc model, as both loss of 15-LOX2 expression and gain of Myc expression are observed at early stages of PCa development. Furthermore, c-Myc is often amplified in advanced human PCa,<sup>24</sup> and c-Myc alone is sufficient to immortalize primary NHP cells,<sup>25</sup> increasing the relevance of the current study to the human disease.

## Results

### 15-LOX2-induced hyperplasia does not progress to carcinoma even in the absence of p53

That transgenic expression of 15-LOX2 in the mouse prostate (which does not express 15-LOX2 or its ortholog 8-LOX<sup>2</sup>) results in mild hyperplasia<sup>18</sup> was unexpected considering the in vitro evidence for its tumor-inhibitory functions.<sup>9</sup> To a certain degree, the hyperplasia-inducing and potential anti-tumor effects of 15-LOX2 are reminiscent of the context-dependent pro- and anti-tumorigenic functions of c-Myc.<sup>26-28</sup> So might 15-LOX2 have any pro-tumorigenic effects? That hyperplasia in the 15-LOX2 Tg prostates does not progress to PIN or adenocarcinoma<sup>18</sup> argues against this possibility. To further clarify this important point, we crossed both fl26 and svb9 Tg lines<sup>18</sup> with *p53*<sup>+/-</sup> or *p53*<sup>-/-</sup> mice. The rationale is that p53 acts as an important senescence checkpoint in mouse, and its allelic loss or complete ablation often allows hyperplasia, induced by oncogene activation or tumor

suppressor loss, to progress to carcinoma or even metastasis. For example, prostate hyperplasia in the *Pten*<sup>+/-</sup> mouse model does not progress further due to p53-dependent induction of senescence.<sup>29</sup> When p53 is knocked out, senescence is blocked, and the hyperplasia in *Pten*<sup>+/-</sup> mouse prostate progresses to invasive PCa.<sup>29</sup> We observed that the 3-mo-old *p53*<sup>+/-</sup> mouse ventral prostates (VP) showed slightly more severe hyperplasia than the 15-LOX2 Tg VP (Fig. S1A and B). However, the VP in 15-LOX2; *p53*<sup>+/-</sup> animals did not show any progression of the hyperplasia to PIN or adenocarcinoma (Fig. S1A and B). In fact, the 15-LOX2; *p53*<sup>+/-</sup> VP showed slightly reduced hyperplasia compared with the *p53*<sup>+/-</sup> VP (Fig. S1A and B). Similarly, there was no significant difference in the severity of hyperplasia in the 3-mo 15-LOX2; *p53*<sup>-/-</sup> VP compared with 15-LOX2 or *p53*<sup>-/-</sup> VP (Fig. S1C; data not shown). We also analyzed 6-mo-old 15-LOX2; *p53*<sup>+/-</sup> and age-matched 15-LOX2 and *p53*<sup>+/-</sup> mice (n = 10 each) and found no significant differences in the levels of hyperplasia among the 3 genotypes (not shown). Overall, these results indicate that the mild hyperplasia in 15-LOX2 Tg prostates does not histologically progress to PIN (or PCa) even with deficiency or loss of p53. They also argue against a pro-tumorigenic effect of 15-LOX2 in vivo in autochthonous animal models.

### 15-LOX2 inhibits early stages (3–6 mo) of Myc-induced prostatic adenocarcinoma

Does 15-LOX2 possess tumor-suppressive properties in an autochthonous animal model? To address this question, we crossed our 15-LOX2fl26 line<sup>18</sup> with the adenocarcinoma-prone Hi-Myc mice.<sup>23</sup> In Hi-Myc mouse model, PIN lesions are observed as early as ~2 wk of age, and by 3 mo 100% of the Tg prostates develop PIN, which then progresses to adenocarcinoma. By 6 mo, 100% of the mice develop invasive PCa characterized by downregulation of laminin and  $\alpha$ -smooth muscle actin ( $\alpha$ -SMA).<sup>23</sup> We have successfully established Hi-Myc;15LOX2fl26 double Tg mice (hereafter referred to as dTg or Myc;LOX; Fig. 1A and B). Both transgenes (15-LOX2 and c-Myc) were expressed mainly in the VP and LP (lateral prostate) with little expression in the DP (dorsal prostate) and undetectable expression in the AP (anterior prostate) (Fig. 1B).

We first analyzed the PIN and tumor phenotypes in 3-mo-old Hi-Myc and dTg prostates (Figs. 1C and 2). Several dozens of 3-mo-old Hi-Myc mice examined showed extensive PIN lesions in their dorsolateral (DLP) and VP lobes as determined by both IHC (Fig. 1C) and Aperio ScanScope-based imaging analysis of whole-mount (WM) sections (Fig. 2). Interestingly, a few 3-mo-old Hi-Myc animals (e.g., WM91; Figs. 1C and 2) also showed progression of PIN to adenocarcinoma. Remarkably, in 3-mo-old Myc;LOX animals, only moderate induction of PIN with the involvement of very few glands was observed (Figs. 1C and 2). Cribriform structures/tufting or nuclear atypia characteristic of PIN<sup>30</sup> were seen less frequently, and overall severity of the lesions was much less conspicuous in the dTg prostates compared with Hi-Myc prostates (Figs. 1C and 2; data not shown).

We subsequently analyzed tumor development and progression in ~6-mo-old prostates (Figs. 3 and 4; Fig. S2). At 6 mo, the Hi-Myc prostatic lobes were much larger than wild-type (Fig. 3A) or 15-LOX2 (not shown) prostates. Strikingly, the

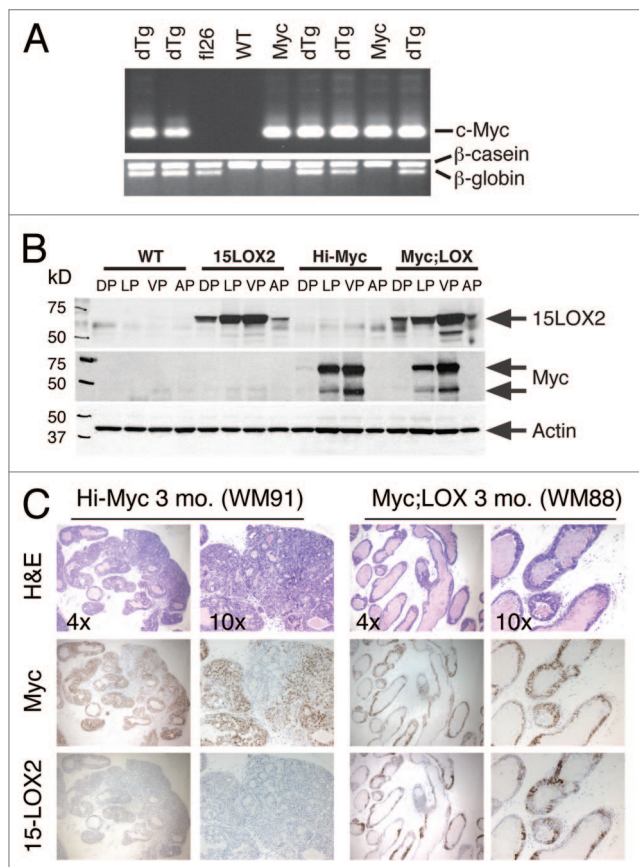


**Figure 1.** Characterizations of Myc;LOX transgenic mice and tumor inhibition by 15-LOX2. **(A)** Genomic PCR genotyping of single and dTg animals using  $\beta$ -globin for 15-LOX2 transgene (f126),<sup>18</sup> c-Myc for Hi-Myc transgene,<sup>23</sup> and  $\beta$ -casein as internal control. WT, wild-type; f126, 15-LOX2f126 Tg; Myc, Hi-Myc; dTg, Myc;LOX dTg. **(B)** Western blot analysis of 15-LOX2 and Myc expression in single and dTg prostate lobes harvested from 3-mo-old animals of the genotypes indicated. **(C)** Representative whole-mount (WM; animal number indicated in the parentheses) dorsolateral (DLP) prostate HE, and Myc and 15-LOX2 IHC images of Hi-Myc vs. dTg (Myc;LOX) animals at 3 mo. Note that Hi-Myc mouse prostate lacks 15-LOX2 staining and Myc;LOX prostate lobes lack PIN and cancer lesions prevalent in Hi-Myc mice. Original magnifications of the objective lens were indicated.

6-mo-old Myc;LOX prostates were nearly the same size as the WT counterparts (Fig. 3A). When the VP and DLP lobes from 6-mo-old WT, f126, Myc, and Myc;LOX mice were micro-dissected out, although the weights of WT and f126 VP plus DLP did not differ significantly, the weights of Hi-Myc lobes doubled (Fig. 4A). Remarkably, the combined VP plus DLP weights in Myc;LOX mice were significantly reduced compared with the Hi-Myc lobes (Fig. 4A). Histologically, the 6-mo-old Hi-Myc mice showed adenocarcinoma in 100% of the mice with nearly 100% involvement of LP, whereas the Myc;LOX animals showed far less adenocarcinoma with fewer glands involved (Fig. 3B). The tumor-suppressive effects of 15-LOX2 were most evident in analysis of WM sections (see representative images in Fig. 4C; Fig. S2). We employed a novel quantification method of WM sections using Aperio ScanScope. Briefly, we first scanned the HE slides of WM prostate sections from WT, Hi-Myc, and

Myc;LOX mice using Aperio ScanScope with trainable GENIE morphometric software and obtained digital images of the WM sections (note that prostates from 15-LOX2f126 mice were not used in this analysis as significant differences were not observed). These virtual slides were used to quantify the % epithelial area, which is directly proportional to the intensity of adenocarcinoma. When % epithelial areas were measured using this method ( $n > 5$  animals each), significant difference was observed between WT and Hi-Myc and, importantly, between Hi-Myc and Myc;LOX prostates (Fig. 4B and C). These results show that PIN progression to adenocarcinoma was delayed and significantly inhibited in the 6-mo-old Myc;LOX dTg prostates. At 12-mo-of-age, the Hi-Myc tumors became large and prominent, and no significant differences in tumor weights between the Hi-Myc and Myc;LOX prostates were observed (data not shown).

The invasive Hi-Myc adenocarcinoma is characterized by the absence of laminin and  $\alpha$ -SMA,<sup>23</sup> which are the markers of basement membrane and fibromuscular layers, respectively. Numerous nests of acini consisting of atypical cells extend into the stroma and exhibit crowding, irregular contours, and haphazard growth patterns.<sup>23</sup> When 6-mo-old Hi-Myc and Myc;LOX prostates were stained for laminin and  $\alpha$ -SMA, the Hi-Myc prostates showed micro-invasions and discontinuous or loss of laminin and  $\alpha$ -SMA expression (Figs. S2 and S3; data not shown). In contrast, the Myc;LOX prostates showed mostly a continuous laminin and  $\alpha$ -SMA expression pattern, and micro-invasions were rarely observed (Figs. S2 and S3; data not shown).

To determine whether the tumor-suppressive properties of 15-LOX2 at early stages (3–6 mo) require its AA-metabolizing enzymatic activity, we crossed the 15-LOX2svb (svb9) transgenic line, which expresses an inactive 15-LOX2 that does not metabolize AA,<sup>18</sup> with the Hi-Myc mice to generate Hi-Myc;15LOX2svb9 (i.e., Myc-svb9) dTg line. When we analyzed Myc-svb9 mice at 3 and 6-mo-of-age ( $n \geq 5$  at each age), we did not see any decrease in levels of PIN or adenocarcinoma compared with Hi-Myc mice (data not shown). These observations imply that the 15-LOX2 enzymatic activity is necessary for its tumor-inhibitory activity *in vivo*.

A pilot qPCR analysis of murine 8-LOX mRNA in the 3-mo-old prostates did not detect its mRNA expression in either WT or 15-LOX2f126 or dTg animals (data not shown), consistent with earlier reports that 8-LOX is not expressed in the mouse prostate.<sup>5</sup>

#### Evidence that 15-LOX2 expression is inversely correlated with c-Myc expression in human PCa

Since both 15-LOX2 and c-Myc transgenes are driven by the ARR2Pb promoter and are thus expressed in the same cell type, our observations that 15-LOX2 co-expression suppressed early stages of Hi-Myc tumor development suggest certain functional antagonism between the 2 molecules. To determine the potential relevance of these observations to human PCa (HPCa), we performed an IHC analysis of 15-LOX2 and c-Myc expression in serial sections of 10 HPCa (T) and the matched normal (N) tissues, and we observed interesting reciprocal expression patterns of the 2 molecules (Fig. 5A and B; Fig. S4; data not shown). Normal prostatic tissues expressed cytoplasmic 15-LOX2 protein but little or very low levels of nuclear c-Myc

(Fig. 5A and B, panels a and b; Fig. S4). In contrast, in HPCa, 15-LOX2 protein expression was generally lost, whereas c-Myc expression was elevated (Fig. 5A, panels d, e, g, and h; Fig. 5B, panels d and e; Fig. S4). The inverse correlation between 15-LOX2 and c-Myc was most vividly illustrated in tumor vs. benign areas in the same HPCa sample (e.g., Fig. 5A, panels d and e). These results are consistent with the reported loss of 15-LOX2 (refs. 6, 8, 14, and 15) and overexpression of c-Myc (ref. 23) in HPCa.

We also analyzed several PCa data sets from Oncomine to explore the relationship between 15-LOX2 and c-Myc mRNAs. As illustrated from the results of 2 such data sets, i.e., Liu et al. (Fig. 5C; ref. 31) and Taylor et al. (Fig. 5D; ref. 32), there existed a strong inverse correlation between 15-LOX2 and c-Myc mRNA expression. This inverse correlation was particularly striking in the Taylor data set, especially when comparing normal prostate gland and metastasis samples (Fig. 5D).

Altogether, both protein and mRNA analysis (Fig. 3) provides evidence that 15-LOX2 and c-Myc are reciprocally expressed in human prostate and prostate cancer tissues.

#### Tumor-suppressive functions of 15-LOX2 in Myc;LOX prostates are associated with increased senescence induction

15-LOX2 expression in primary NHP and PCa cells has been linked to inhibition of cell proliferation and induction of senescence.<sup>7,9,11</sup> Cell senescence acts as an impediment to both tumorigenesis and benign to malignant progression.<sup>9,12</sup> Two PCa animal models vividly illustrate the critical importance of senescence in impeding tumor development. One is the *Pten*<sup>+/-</sup> mouse model, in which prostatic hyperplasia does not progress to PCa due to p53-dependent senescence checkpoint.<sup>29</sup> In the absence of p53, senescence is not induced, and hyperplasia progresses to invasive carcinoma.<sup>29</sup> In the other example, probasin-driven AKT mouse model (MPKAT) “superactivation” of Akt signaling in mouse prostate epithelial cells also leads to hyperplasia and PIN that do not progress to adenocarcinoma due to p27-dependent senescence induction.<sup>33,34</sup> In our 15-LOX2 Tg mice, there was increased cell senescence associated with p27 upregulation.<sup>18</sup> Hence, we hypothesized that early induction of senescence may be responsible, at least partly, for the observed tumor-suppressive effects of 15-LOX2 in Myc;LOX mice. To test this hypothesis, we performed SA- $\beta$ gal staining on cryosections of 3-mo-old Hi-Myc and Myc;LOX prostates along with age-matched WT and fl26 prostates. As exemplified in Figure 6A, there was a noticeable increase in SA- $\beta$ gal-positive glands in fl26 prostates compared with WT prostates, as previously observed.<sup>18</sup> Important, there were also significantly more SA- $\beta$ gal-positive glands in the prostates of Myc;LOX animals compared with Hi-Myc mouse prostates (Fig. 6A). As increase in p27 expression was associated with

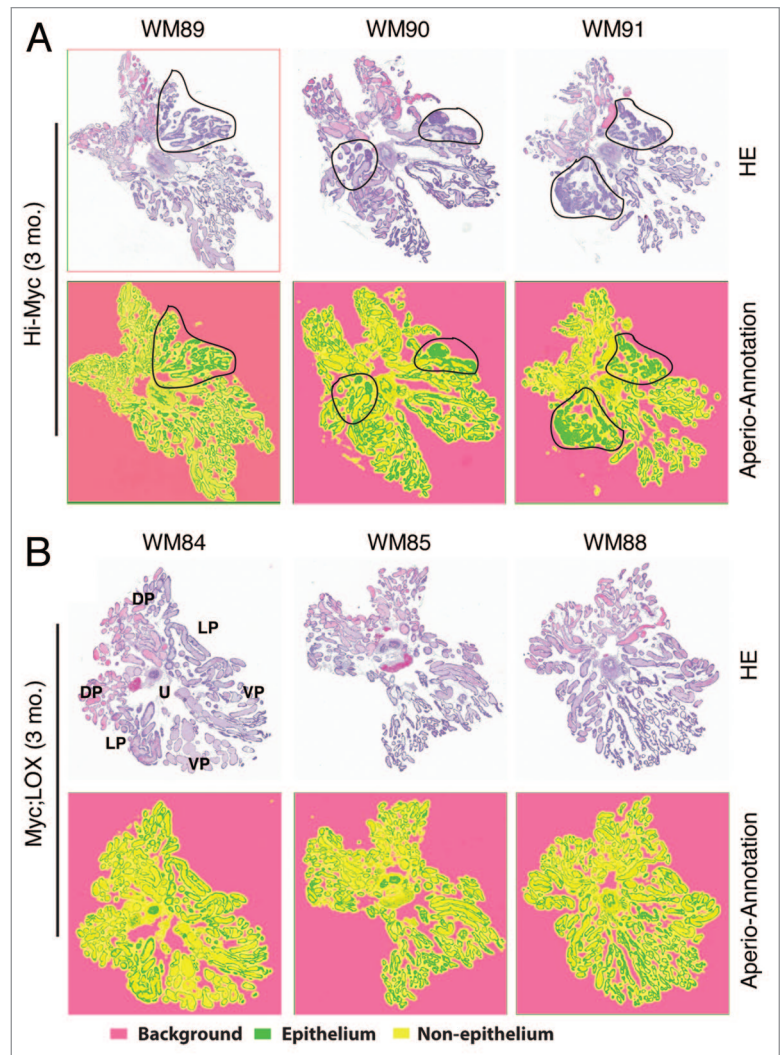


**Figure 2.** Inhibition of PIN and tumor development in 3-mo-old Myc;LOX transgenic mice. **(A)** WM prostates from 3 representative 3-mo-old Hi-Myc animals (total n = 15). Shown are HE (top) and the corresponding Aperio ScanScope (below) images. The areas demarcated by black lines indicate the PIN and early adenocarcinoma lesions. The WM numbers are indicated on top. **(B)** WM prostates from 3 representative 3-mo-old Myc;LOX dTg animals (total n = 7). Shown are HE (top) and the corresponding Aperio ScanScope (below) images. The orientation of the WM is illustrated on the HE image of WM84. U, urethra; DP, dorsal prostate; LP, lateral prostate; VP, ventral prostate. The virtual slides shown below were generated with Aperio ScanScope with trainable GENIE morphometric software that permits morphometric quantification of scanned images. The color coding was indicated below. Note that the histological presentations of WM91 and WM88 at higher magnifications are shown in Figure 1C.

15-LOX2-induced senescence,<sup>18</sup> we performed western blotting analysis to examine whether p27 levels are elevated in 3-mo-old Myc;LOX mice. The results revealed increased p27 in all prostatic lobes of 15-LOX2fl26 mice as well as in the VP and DLP lobes of Myc;LOX mice compared with Hi-Myc lobes (Fig. 6B).

Since cell senescence is well known to involve Rb-mediated cell cycle arrest, we examined the Rb levels in the 3 mo Myc;LOX prostates. This preliminary study revealed very interesting differences in total Rb and inactive Rb (i.e., Phos-Rb; phosphorylated

on ser-780) protein levels in different prostatic lobes (Fig. 6C). In WT prostates, total Rb protein was observed in VP > LP > AP >> DP, whereas Phos-Rb was observed mainly in LP and VP (Fig. 6C). In 15-LOX2fl26 prostates, total Rb protein was observed in VP > AP > DP >> LP, but Phos-Rb was observed mainly in LP and VP (Fig. 6C). Interestingly, the Phos-Rb (i.e., inactive Rb) levels were increased in 15-LOX2fl26 prostates (Fig. 6C) compared with the WT prostates, consistent with our earlier observations of a hyper-proliferative phenotype in the former.<sup>18</sup> In Hi-Myc as well as in Myc;LOX2 prostates, both total and Phos-Rb were observed prominently in LP and VP (Fig. 6C). Strikingly, the inactive Rb levels were reduced in dTg prostates in comparison to both 15-LOX2fl26 and Hi-Myc prostates (Fig. 6C), which could potentially contribute to the observed tumor-suppressive functions of 15-LOX2. Together, the results on p27 (Fig. 6B) and Rb (Fig. 6C) suggest that 15-LOX2-mediated tumor suppression in Hi-Myc model might involve cell senescence induction associated with molecular changes in these 2 molecules.

### 15-LOX2 metabolites induce RB1CC1 in normal human prostate (NHP) and RWPE1 cells

One of the intriguing earlier findings is that the mouse *Rb1cc1* mRNA and protein are induced in the 15-LOX2fl26 Tg prostates.<sup>18</sup> Indeed, we corroborated this upregulation in a new cohort of WT

and 15-LOX2fl26 Tg animals (Fig. 6D). Of interest, elevated levels of *Rb1cc1* mRNAs were also observed in Myc;LOX prostates compared with the Hi-Myc prostates (Fig. 6D). *Rb1cc1*, which is an Rb1 inducible protein and can also induce Rb1, has been linked to inhibition of cell proliferation and induction of senescence in several cell systems.<sup>18-21,35</sup> We thus followed up on this observation by determining the potential interrelationships among 15-LOX2, human RB1CC1, and prostate epithelial cell senescence (Fig. 7). To this end, we generated NHP60 cells (from the uninvolved benign tissue of primary PCa patient #60 using methods previously described<sup>10-12</sup>) and passaged them for up to 5 passages. Semi-quantitative RT-PCR (Fig. 7A) and qPCR (Fig. 7B) revealed increasing RB1CC1 mRNA levels in NHP60 cells as a function of increasing passages. The serially passaged NHP60 cells were undergoing replicative cell senescence as evidenced by increasing levels of p16INK4A (p16) (Fig. 7C), a critical negative cell cycle regulator of and a senescence hallmark protein for cultured NHP cells.<sup>12</sup> These results suggest that RB1CC1, similar to 15-LOX2, accumulates in NHP cells undergoing senescence.

The fact that increased *Rb1cc1* expression was observed in 15-LOX2fl26 animals, which produce enzymatically active 15-LOX2 but not in WT or in 15-LOX2svb, which is enzymatically inactive,<sup>18</sup> suggests that 15-LOX2 metabolites may be mediating the *Rb1cc1* induction. To test this connection in NHP cells, we treated NHP60 cells (P3) with the 15-LOX2 metabolite 15(S)-HETE for 24 h and 48 h and then analyzed RB1CC1 expression by immunofluorescence. As shown in Figure 7D, in NHP60 cells treated with vehicle (ethanol) for 48 h, there were only scattered RB1CC1-positive cells. In contrast, in NHP60 cells treated with 15(S)-HETE (5  $\mu$ M; the main metabolite of 15-LOX2) for 24 h, many turned strongly positive for RB1CC1, and some RB1CC1-positive cells were noticeably flat, large, and most likely senescent (Fig. 7D). At 48 h, most 15(S)-HETE-stimulated NHP60 cells stained positive for RB1CC1 (Fig. 7D). Of note, many of the 15(S)-HETE-treated NHP60 cells showed strong nuclear RB1CC1 staining (Fig. 7D, red arrows).

Due to limited numbers and lifespan of cultured primary NHP cells,<sup>9-12</sup> we subsequently used RWPE-1, an immortalized prostate epithelial cell line, to further investigate whether 15-LOX2 metabolite(s) transcriptionally induce RB1CC1. As shown in Figure 7E, 15(S)-HETE dose-dependently increased the *RB1CC1* mRNA levels. The precursor metabolite to 15(S)-HETE, 15(S)-HPETE, also induced RB1CC1 in a dose-dependent manner (Fig. 7E). 15-LOX2 metabolites were previously shown to induce reactive oxygen species (ROS)<sup>36</sup> and thus can alter the redox balance in the cells. We pretreated RWPE-1 cells with hydrogen peroxide ( $H_2O_2$ ), a potent ROS inducer, and observed that it also induced RB1 as well as RB1CC1. As expected, induction of RB1 and RB1CC1 by  $H_2O_2$  was blocked by the ROS inhibitor N-acetyl cysteine (NAC; Fig. 7E). These observations raised the possibility that the 15-LOX2 metabolite induced RB1 and RB1CC1 expression might also involve ROS production. In support of this possibility, NAC inhibited the inductive effects of 15(S)-HETE and 15(S)-HPETE (Fig. 7E).

15-LOX2 metabolites have been shown to activate the redox transcription factor activating protein-1 (AP-1) in a

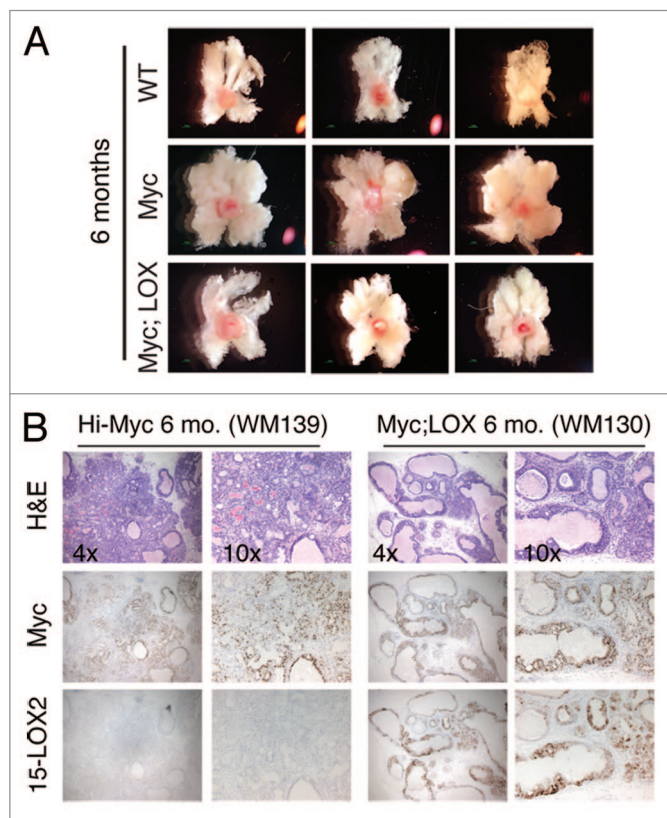


**Figure 3.** 15-LOX2 inhibits Hi-Myc tumor development in 6-mo-old animals. (A) WM prostates (including DLP and VP) from 3 representative animals each of WT (total n = 15), Hi-Myc (n = 7), and 15LOX2fl26;Hi-Myc (n = 7) genotypes at 6 mo. (B) Representative HE and Myc vs. 15LOX2 IHC images of Hi-Myc and Myc;LOX prostates at 6 mo. Original magnifications of the objective lens were indicated.

ROS-dependent manner.<sup>37</sup> c-FOS and c-JUN dimerize in various combinations to form the AP-1 complex. We tested whether there might be an association between 15-LOX2 metabolite treatment and AP-1 induction in RWPE-1 cells. As shown in Figure 7E, both 15(S)-HETE and 15(S)-HPETE upregulated the mRNA levels of c-FOS and c-JUN, which was inhibited by NAC.

#### RB1CC1 is unexpectedly upregulated in most HPCa samples

The preceding experimental results imply certain positive correlations between 15-LOX2, its metabolite 15(S)-HETE, and RB1CC1. This seemed to be the case in the 10 normal human prostate tissues we analyzed (Fig. 5A and B; Fig. S4). For example, in HPCa16N and HPCa11N, the prostatic glands that expressed high 15-LOX2 tended to also show strong RB1CC1 staining (Fig. 5A and B; Fig. S4). Since 15-LOX2 expression is undetectable in >20 immortalized prostate epithelial and PCa cell lines<sup>7-9,12</sup> and downregulated or lost in the precursor lesion HGPIN as well as >70% HPCa samples,<sup>7,9,15,16</sup> we wondered whether RB1CC1 might also be reduced or lost in PCa cells *in vitro* and *in vivo*. To our surprise, the *RB1CC1* mRNA levels were actually elevated in several PCa cell lines in comparison to NHP60 cells (Fig. 8A). Examination of 15 Oncomine data sets (ref. 38; data not shown) revealed that the *RB1CC1* mRNA levels were increased in HPCa compared with normal prostate tissues (Fig. 8B and C). In fact, the *RB1CC1* mRNAs were increased even more prominently in the precursor lesion PIN, although its levels were not altered in the benign prostate hyperplasia (BPH)

samples (Fig. 8B). IHC analysis of RB1CC1 protein also revealed that in contrast to 15-LOX2, RB1CC1 was detected or elevated in the 10 HPCa samples examined (Fig. 5A and B; Fig. S4; data not shown).

#### RB1CC1 knockdown promotes PC3 cell clonal and tumor growth

Might the RB1CC1 that was overexpressed in PCa cells possess tumor-suppressive functions as previously reported in case of breast cancer?<sup>39</sup> We addressed this question by generating PC3 cells with RB1CC1 stably knocked down, as verified by both qRT-PCR (Fig. 9A) and western blotting (Fig. 9B) analyses. Strikingly, RB1CC1 knockdown greatly promoted PC3 clonal growth (Fig. 9C–E). Early (*i.e.*, 3 d) after plating, although control non-silencing (NS) vector transduced PC3 cells frequently existed as large, isolated single or double cells, the RB1CC1 knocked down PC3 cells founded numerous clones that contained small, fast proliferating cells (Fig. 9D). When plated at clonal density (*i.e.*, 100 cells/well) and observed at the end of 2 wk, both PC3 cell types with RB1CC1 knocked down formed significantly more clones than the NC or GAPDH-shRNA vector transduced PC3 cells (Fig. 9C and E). Consistent with the clonal-promoting effects, RB1CC1 knockdown also accelerated the emergence and growth rate of PC3 xenograft tumors in NOD/SCID mice (Fig. 9F–G). These loss-of-function studies suggest that RB1CC1 possesses PCa-suppressive functions. In support of this suggestion, preliminary gain-of-function studies in several NHP strains revealed that

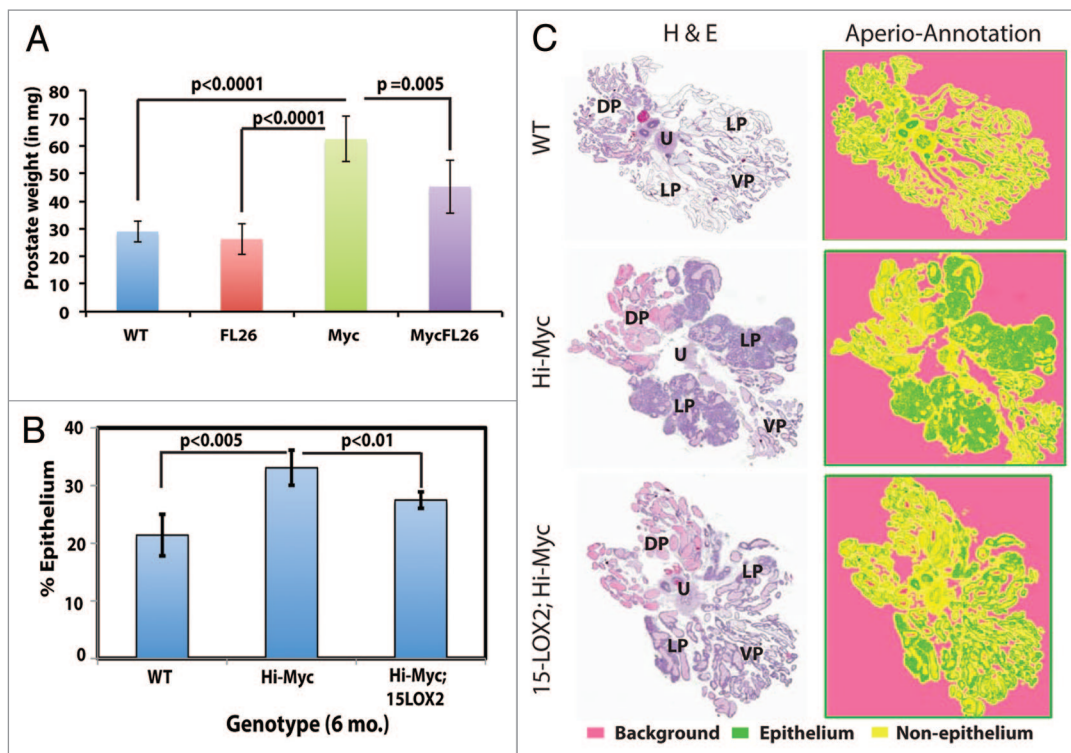


**Figure 4.** 15-LOX2 suppresses Hi-Myc adenocarcinoma in 6-mo-old dTg animals. (A) Prostate weight comparisons of WT and Tg animals. DLP and VP lobes of mice ( $n \geq 7$ ) from respective genotypes were dissected out, and collective weights of the lobes measured. (B) Quantification of epithelial tumor areas. Shown are the mean epithelial area (%) quantified from WM prostate sections in WT ( $n = 5$ ), Hi-Myc ( $n = 7$ ) and Hi-Myc;15-LOX2 ( $n = 5$ ) mice using the ScanScope images. (C) Representative H&E images of samples used for quantifications in (B) and the virtual slides generated with Apero ScanScope with trainable GENIE morphometric software that permits morphometric quantification of scanned images. For HE sections, the 4 prostatic lobes and urethra (U) were indicated. For the virtual slides (right), the color coding was indicated below.

overexpression of RB1CC1 caused NHP cell growth arrest, senescence, and/or apoptosis (Fig. S5; data not shown).

## Discussion

We have made the following novel findings in the present study. First, 15-LOX2-induced mild prostatic hyperplasia does not progress to PIN or PCa even in the absence of tumor suppressor p53. Second, 15-LOX2 inhibits early stages of Hi-Myc PCa development. Third, in HPCa, 15-LOX2 and c-Myc manifest reciprocal protein expression patterns. Fourth, 15-LOX2-suppressed Hi-Myc PCa development involves cell senescence induction associated with alterations of p27, Rb, and Rb1cc1. Fifth, RB1CC1 accumulates in senescing NHP cells, and in both NHP and RWPE-1 cells, the 15-LOX2 metabolic products 15(S)-HPETE and 15(S)-HETE induce RB1CC1. Sixth, in benign prostate tissues RB1CC1 and 15-LOX2 demonstrate concordant expression patterns, but in HPCa, 15-LOX2 is lost,

whereas RB1CC1 is, unexpectedly, frequently overexpressed. Finally, RB1CC1 knockdown in PC3 cells enhances clonal growth in vitro and tumor growth in vivo. Together, these findings report tumor-suppressive functions for both 15-LOX2 and RB1CC1.

We recently reported the surprising findings that transgenic expression of 15-LOX2 in the mouse prostate causes mild hyperplasia,<sup>18</sup> implying a potential tumor-promoting effect of 15-LOX2. Nevertheless, this mild hyperplasia does not spontaneously advance to more severe pathological phenotypes such as PIN or adenocarcinoma, with hundreds of animals tracked continuously for >3 y<sup>18</sup> (data not shown). In fact, even when p53, a major molecular mediator of senescence checkpoint, is deleted, 15-LOX2 overexpression-induced hyperplasia fails to progress to more advanced pathological stages. If anything, 15-LOX2 expression actually inhibits the hyperplasia observed in p53<sup>+/-</sup> prostates. This latter observation is consistent with potential tumor-suppressive functions we (see “Introduction”) and others<sup>40</sup> have previously observed. The direct evidence supporting

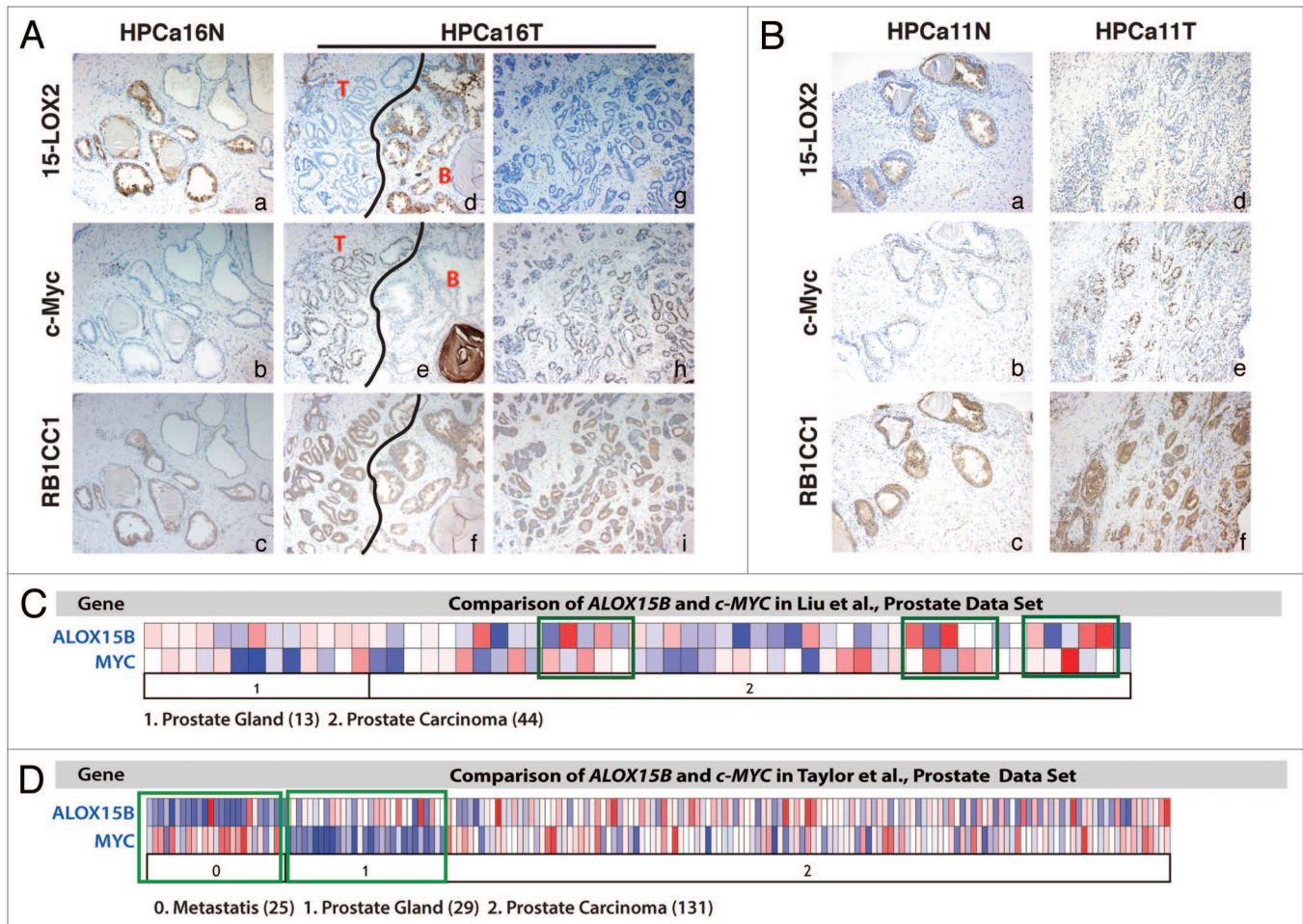


**Figure 5.** Reciprocal and contrasting expression patterns of 15-LOX2 vs. c-Myc and 15-LOX2 vs. RB1CC1 in HPCa samples. (A) Shown are representative images of 15-LOX2, c-Myc, and RB1CC1 IHC in serial sections of HPCa16 (PCa patient sample #16; N and T refer to normal and tumor tissues, respectively). In panels (d–f), the black line demarcates tumor (T) and benign (B) areas. Original magnifications,  $\times 100$ . (B) Shown are representative images of 15-LOX2, c-Myc, and RB1CC1 IHC in serial sections HPCa11. Original magnifications,  $\times 100$ . (C and D) Oncomine data sets in Liu et al. (C; ref. 31) and Taylor et al. (D; ref. 32) showing reciprocal expression of 15-LOX2 (*ALOX15B*) and *c-MYC* mRNAs in benign prostate (prostate gland), prostate carcinoma, and metastatic samples. The numbers of cases are shown in parentheses. Green boxes highlight samples that showed a strong inverse correlation.

tumor-suppressive functions of 15-LOX2 comes from our studies of the Myc;LOX dTg mice. Although the 3-mo Hi-Myc prostates develop prominent PIN lesions and occasional adenocarcinomas, and 100% of the 6-mo Hi-Myc prostates develop full-blown adenocarcinomas, 15-LOX2 co-expression remarkably inhibits both PIN and tumor phenotypes at both time points. Tumor-inhibitory effects of 15-LOX2 are no longer observed in the 12-mo-old dTg prostates presumably due to the dominant oncogenic power of c-Myc overexpression and overwhelming volumes of Hi-Myc tumors developed at this late stage. Also, a tumor-inhibitory effect is not observed in crosses between 15-LOX2svb9 and Hi-Myc, implying a requirement for 15-LOX2 metabolites in mediating the tumor-suppressing functions of 15-LOX2.

How might 15-LOX2 expression inhibit c-Myc induced prostate tumor development? Intriguingly, 15-LOX2 and c-Myc seem to display reciprocal expression patterns at both the mRNA and protein levels. Since upregulation of c-Myc and loss of 15-LOX2 both occur early during HPCa development, it is tempting to speculate that c-Myc upregulation may transcriptionally repress 15-LOX2 expression, and that 15-LOX2, either directly or indirectly (i.e., through its metabolites), may functionally antagonize the c-Myc activity. Future studies will test these speculations. Regardless, the functional antagonism between 15-LOX2 and c-Myc observed in the Hi-Myc model may

involve cell cycle regulation and senescence induction. c-Myc is the only oncogene that, by itself, is sufficient to immortalize primary prostate epithelial cells.<sup>25</sup> On the other hand, 15-LOX2 metabolites induce senescence of both NHP and PCa cells,<sup>9</sup> and 15-LOX2 overexpression promotes cell senescence in NHP cells in vitro<sup>11</sup> and in mouse prostate epithelial cells in Tg animals.<sup>18</sup> Of relevance, prominent cell senescence is also observed in the Myc;LOX dTg prostates, potentially explaining the observed tumor-suppressive functions of 15-LOX2.

In the 15-LOX2fl26 Tg prostates, senescence induction is accompanied by increased p27 and Rb1cc1 expression,<sup>18</sup> and increased expression of these 2 molecules is similarly observed in the Myc;LOX prostates. Notably, we extend the molecular alterations in Rb1cc1 to NHP epithelial cells. Thus, RB1CC1 is upregulated accompanying the NHP cell senescence. We further show that RB1CC1 expression in both NHP and RWPE-1 cells can be induced by 15-LOX2 products 15(S)-HPETE and 15(S)-HETE, possibly involving ROS production and AP-1-mediated transcriptional activation. In support, H<sub>2</sub>O<sub>2</sub> can induce c-FOS/c-JUN and RB1CC1 expression, whereas the ROS inhibitor NAC blocks the expression of these molecules induced by not only H<sub>2</sub>O<sub>2</sub>, but also 15-LOX2 metabolites. Combining the tumor-inhibitory phenotypes in 15-LOX2fl26;Hi-Myc but not in 15-LOX2svb9;Hi-Myc dTg animals and the in vitro studies in NHP and

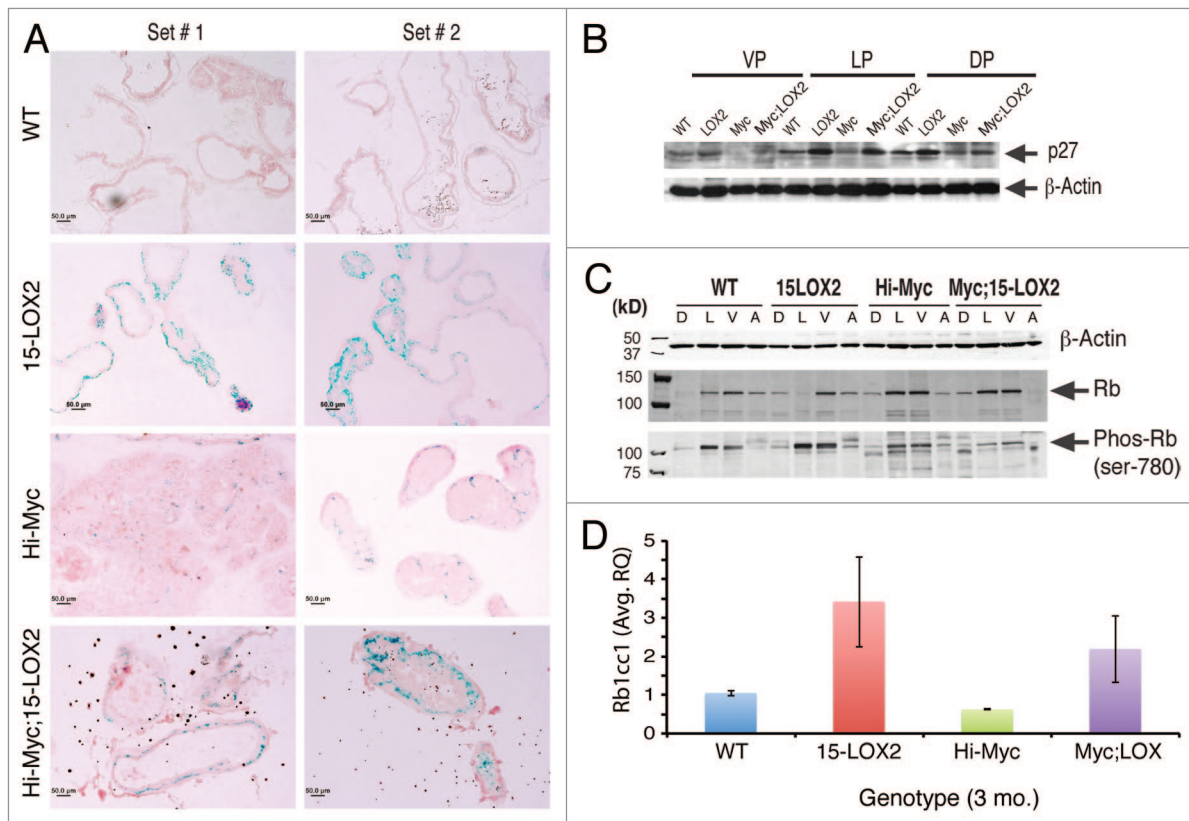


**Figure 6.** Cell senescence in Myc;LOX prostates. (A) Representative SA-βgal staining images in 3-mo-old prostates showing senescence in the Myc;LOX prostates. (B) Western blot analysis showing p27 expression in various prostate lobes of 3-mo mice among different genotypes. β-actin was used as the loading control. (C) Altered Rb1 and Phos-Rb in Myc;LOX prostates. Prostatic lobes were microdissected out from the animals of the indicated genotypes (3 mo) and used in western blotting analysis of the indicated molecules. (D) Increased *Rb1cc1* mRNA expression in 15-LOX2 single or double transgenic prostates. Presented are the mean ± SD data from 2 sets of mice.

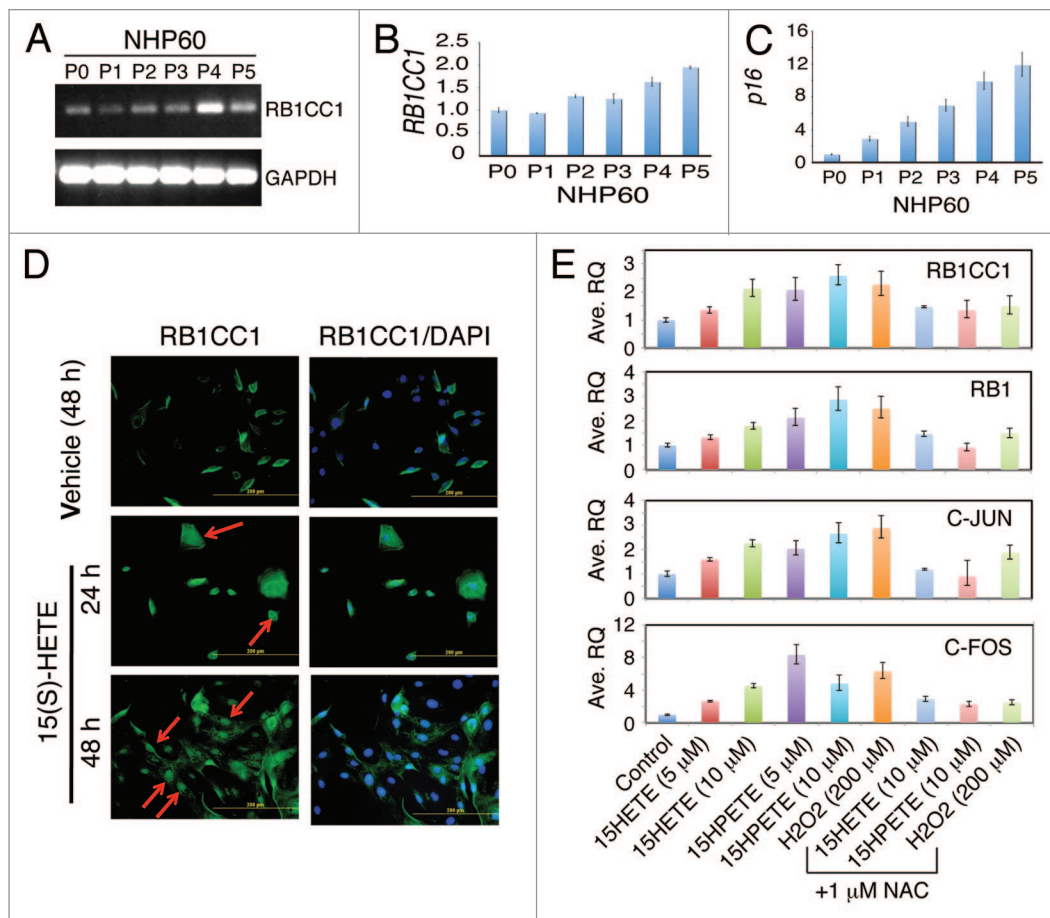


**Figure 7.** Changes of RB1CC1 during NHP cell senescence and upon 15(S)-HETE treatment. (A and B) Increasing *RB1CC1* mRNA levels in serially passaged primary NHP cells. NHP60 cells purified from benign prostate tissue and serially passaged were used in analysis of *RB1CC1* mRNA by either regular RT-PCR (A) or qRT-PCR using ABI Biosystems Taqman assays (B). GAPDH PCR was used as controls. (C) qPCR analysis showing increasing levels of *p16* mRNA in serially passaged NHP60 cells. (D) Induction of RB1CC1 in NHP60 cells by 15-LOX2 metabolite, 15(S)-HETE. NHP60 cells treated with 15(S)-HETE (5  $\mu$ M) were immunostained for RB1CC1. Original magnifications,  $\times 200$ . (E) 15-LOX2 metabolites (15[S]-HETE and 15[S]-HPETE) induce RB1CC1 and other related molecules in RWPE-1 cells. RWPE-1 cells were treated with 15-LOX2 metabolites at the concentrations indicated and the mRNA levels of the indicated molecules were analyzed by qPCR. In some conditions, cells were pretreated with  $H_2O_2$  (200  $\mu$ M) or NAC (1 mM). Shown are the mean  $\pm$  SD from 2 independent measurements.

RWPE-1 cells, we hypothesize that 15-LOX2 overexpression leads to overproduction of 15-HPETE and 15(S)-HETE (as demonstrated earlier<sup>18</sup>), which then induce upregulation of RB1CC1, partially via oxidative stress-induced AP1 induction/activation. RB1CC1, by activating RB (ref. 41) or p16 (ref. 42) may, in turn, contribute to induction of cell senescence.

The above hypothesis predicts a concordant relationship between 15-LOX2 and RB1CC1 in NHP cells, and this seems to be the case even for benign prostate tissues *in vivo*. Unexpectedly, however, discordant expression between the 2 molecules is observed in PCa cells *in vitro* and *in vivo*: whereas 15-LOX2 expression is generally lost, the RB1CC1 expression remains in HPCa. In fact, RB1CC1 appears to be overexpressed in a significant fraction of HPCa samples. Nonetheless, knockdown studies in PC3 PCa cells still reveal a powerful tumor-suppressive function of RB1CC1, just as previously reported in breast cancer cells.<sup>39</sup> Since RB1CC1 interacts with many partners, it is possible that retention or overexpression of RB1CC1 in PCa represents a

consequence of some of these interactions. To a certain degree, overexpression of RB1CC1 in PCa but still acting as a tumor suppressor is akin to LRIG1, a well-known stem cell marker elevated in PCa but found to inhibit PCa cell proliferation.<sup>43</sup> Future studies will further delineate RB1CC1 as a potential mediator of the 15-LOX2 tumor-suppressive functions.

## Materials and Methods

### Animal experiments

Basic procedures in producing and propagating transgenic animals have been previously described.<sup>18,44</sup> 15-LOX2 Tg animals were crossed to Hi-Myc animals to produce Hi-Myc;15-LOX2fl26 and Hi-Myc;15-LOX2svb9 dTg animals. Hi-Myc animals were obtained from J DiGiovanni lab. Genotyping for 15-LOX2 animals was performed as reported earlier<sup>18</sup> using  $\beta$ -globin and  $\beta$ -casein primers and genotyping for Myc using

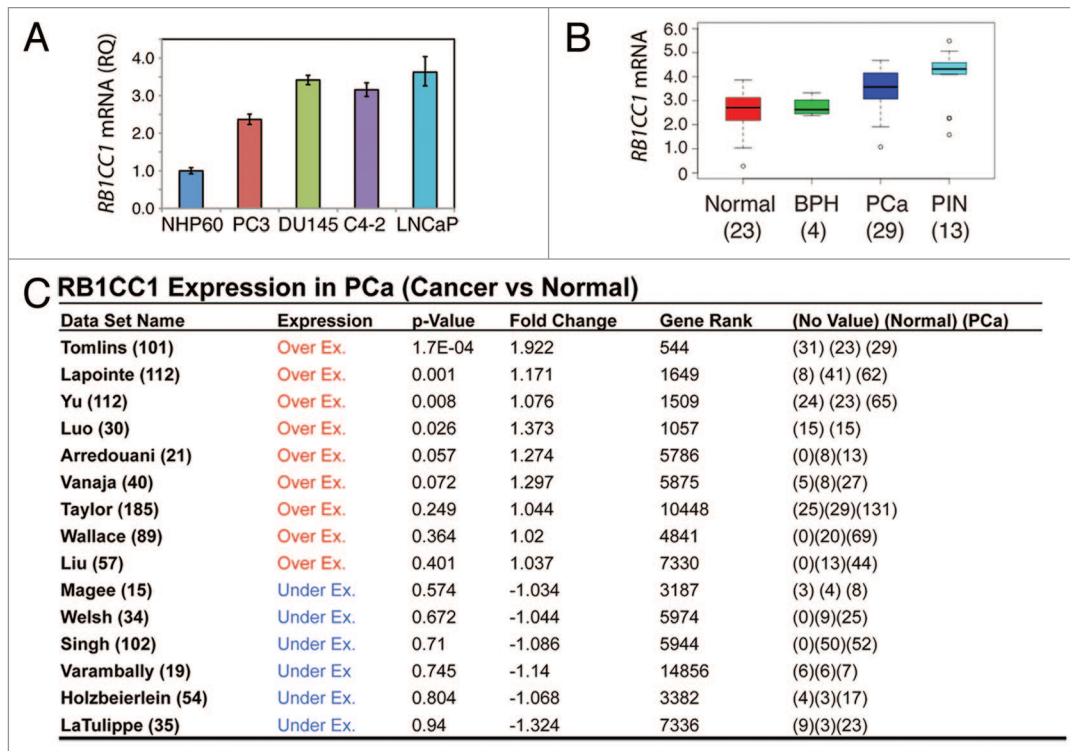


**Figure 8.** Unexpected (over)expression of RB1CC1 in PCa cells and HPCa samples. (A) qRT-PCR analysis showing increased *RB1CC1* mRNA levels in PCa cells compared with NHP60 cells. (B) Elevated *RB1CC1* mRNA levels in PIN and HPCa samples. The relative mRNA expression values were summarized from Tomlins et al. (ref. 38). (C) Elevated *RB1CC1* mRNA levels in the majority of the 15 Oncomine data sets. In the first column, the total number of cases was indicated. In the last column, numbers in parentheses indicate the numbers for no value, normal, and PCa, respectively.

primers as described.<sup>23</sup> 15-LOX2 animals were crossed to either p53<sup>-/-</sup> or p53<sup>+/-</sup> to obtain 15-LOX2; p53<sup>+/-</sup> and 15-LOX2; p53<sup>-/-</sup> animals. All procedures involving the usage of animals were approved by the IACUC.

#### Point-sampled intercepts method to quantify epithelial hyperplasia

The point-sampled intercepts method<sup>45,46</sup> was used to quantify epithelial hyperplasia in 15-LOX2 and p53 single and compound mice. Briefly, 2 VP images were captured at 100× using a Nikon Digital Sight camera attached to an Olympus BX40 microscope. The images were imported into Adobe Photoshop at full size and viewed with a millimeter grid overlay (view > show > grid). The image was captured from the screen as a .png file using the shift/apple/4 command; incomplete squares were not included. The image was printed in black and white at full size (2400 × 1800 pixels at 300 pixels per inch). A positive point consisted of the intersection of 2 major grid lines overlying epithelium.

#### Slide scanning with Aperio ScanScope microscope and prostate adenocarcinoma quantification using trainable Genie morphometric software

HE-stained or immunostained slides were scanned using the Aperio ScanScope imaging platform (Aperio Technologies) with a 20× objective at a spatial sampling period of 0.47 μm per pixel. Whole-slide images (WSI) were viewed with ScanScope software. A custom GENIE classifier algorithm was trained to discriminate between prostate epithelium and stroma and to score and quantify each area. Total area was recorded for each of the

structures detected by the algorithm, and data were presented as % epithelium of the total scored area of each slide. Slides from WT, Hi-Myc, and Myc;LOX animals were included in the analysis.

#### Cell culture

PC3 and RWPE1 cells were obtained from ATCC and cultured, respectively, in RPMI supplemented with 7% heat-inactivated FBS and antibiotics and keratinocyte basal medium (KBM) supplemented with necessary growth factors (Lonza). Normal human prostate (NHP) cells were derived following the procedure published previously by our group.<sup>8,10-12</sup> The derived NHP cells, NHP55, NHP57, NHP60, and NHP146, were propagated in prostate epithelia basal medium (PrEBM) supplemented with necessary growth factors (Lonza) and used in various experiments.

#### Transfection and generation of stable RB1CC1 knockdown PC3 cells

Stable knockdown cell lines were generated by transfecting PC3 cells with pGIPZ vectors (Open Biosystems) for RB1CC1 (Clone ID #1 V3LHS-307113; Clone ID #2 V3LHS-229368), non-silencing (NS), and GAPDH using Arrest-In Transfection Reagent (Open Biosystems), followed by puromycin selection. These cell lines were named PC3-NS, PC3-GAPDH, PC3-RB1CC#1, and PC3-RB1CC#2. Expression of RB1CC1 and GAPDH in knockdown cells was analyzed by qPCR. RB1CC1 knockdown was also confirmed by western blot using a polyclonal antibody raised against the c-terminal region (Sigma; SAB4200135). HEK293T

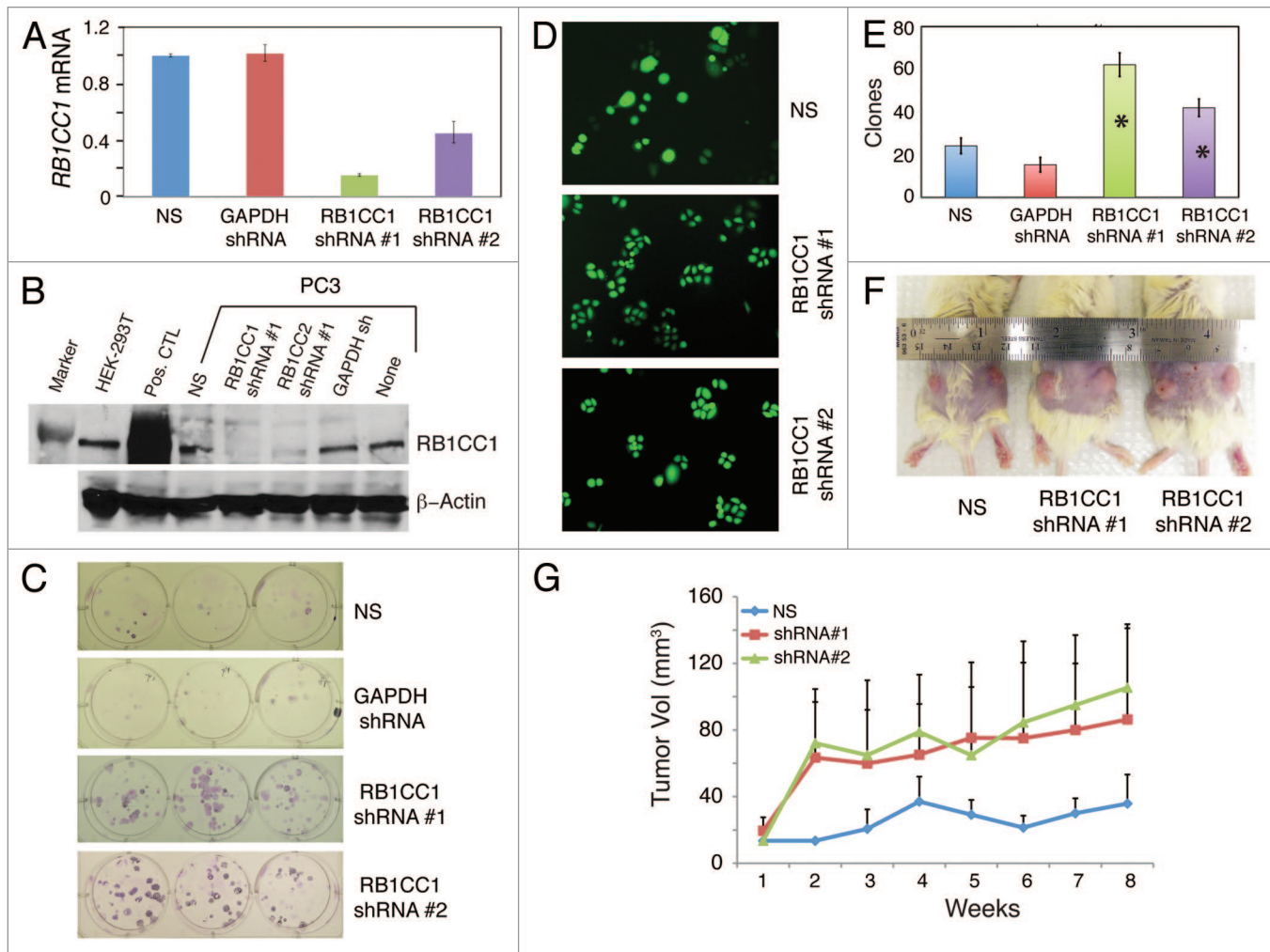


**Figure 9.** RB1CC1 knockdown promotes PC3 cell clonal and tumor growth. **(A)** Confirmation of RB1CC1 knockdown by qRT-PCR. PC3 cells were transfected with non-silencing (NS), GAPDH, or 2 RB1CC1 shRNA lentiviral vectors, and cells were then selected with puromycin to generate stable cell lines, from which total RNA was isolated for qRT-PCR analysis of RB1CC1 mRNA. **(B)** Confirmation of RB1CC1 knockdown by western blot analysis using an antibody from Sigma (# SAB4200135). Both PC3 and HEK-293T cells express endogenous RB1CC1 protein (~200 kD). The positive control (Pos. CTL) lane were HEK293T cells transfected with an RB1CC1-overexpressing plasmid. **(C–E)** RB1CC1 knockdown promotes PC3 cell clonal growth. The 4 types of stably selected PC3 cells were plated at clonal density (100 cells/well) in 6-well plates and images were captured at the end of 3 d **(D)** or 2 wk **(C)**; giemsa stain. Shown in **(E)** is quantification of clones at the end of one week (mean ± S.D.; n = 3). \**P* < 0.001 (compared with NS or GAPDH conditions). **(F and G)** RB1CC1 knockdown promotes PC3 xenograft tumor growth in NOD/SCID mice. The 3 types of stably selected PC3 cells as shown were subcutaneously injected (500 000 cells/injection) into dorsal flanks of 6-wk-old NOD/SCID mice (n = 10 injections/cell type), and the volume measurements were taken on a weekly basis **(G)**. Shown in **(F)** are representative tumor images of each cell type.

and HEK293T transfected with p3XFLAG-CMV10-hFIP200 expression vector (Addgene) were used as controls.

#### Clonal assays and tumor transplantation experiments

For clonal assays,<sup>48</sup> the 4 stable PC3 cell lines were plated at a clonal density (i.e., 100 cells/well) in a 6-well dish and clones counted 1–2 wk later after Giemsa staining. At least one 6-well plate per cell type was used for counting, and the experiment was repeated 3 times. Data were presented as the cloning efficiency for each cell type. To test the effect of RB1CC1 knockdown on tumor growth, we injected PC3-NS, PC3-RB1CC1#1, and PC3-RB1CC1#2 cell lines in 50% Matrigel subcutaneously on each side (500 K/injection) of the dorsal flank of NOD/SCID mice (10 injections/cell type). Tumor measurements were performed

weekly for up to 6 wk using a Vernier caliper, and volumes were calculated using the equation  $\text{volume} = \text{width}^2 \times \text{length} / 2$ .

#### SA-βGal staining, immunohistochemistry (IHC), real-time PCR (qRT-PCR), and western blot

These procedures have been described in our earlier publications.<sup>12,13,18,47</sup> Information for antibodies and qPCR analysis is presented in **Tables S1 and 2**, respectively.

#### Oncomine data analysis

Data analysis of Oncomine database (Compendia Bioscience) was performed to determine: (1) RB1CC1 expression in PCa samples compared with normal tissues from all the expression data sets; and (2) co-expression of c-Myc and 15-LOX2 in PCa vs normal. RB1CC1 expression was obtained from 15 PCa data sets

(see Fig. 8C) and *P* value, fold change, and gene rank values were extracted. Similar co-expression analysis was performed with various PCa data sets available in OncoPrint and results from representative data sets were presented.

#### Disclosure of Potential Conflicts of Interest

No potential conflicts of interest were disclosed.

#### Acknowledgments

We thank L Coletta and J Repass for qPCR analysis, C Perez for Aperio ScanScope analysis, and N Otto and JL

Brandon for IHC. We also thank D Johnson for sharing p53-null mice, and SM Fischer, JL Guan, and other members of the Tang lab for valuable suggestions and assistance during the course of this project. This work was supported, in part, by grants from NIH (R01-CA155693), Department of Defense (W81XWH-13-1-0352), and CPRIT (RP120380), and the MDACC Center for Cancer Epigenetics (D.G.T.).

#### Supplemental Materials

Supplemental materials may be found here: [www.landesbioscience.com/journals/cc/article/28757](http://www.landesbioscience.com/journals/cc/article/28757)

#### References

- Brash AR, Boeglin WE, Chang MS. Discovery of a second 15S-lipoxygenase in humans. *Proc Natl Acad Sci U S A* 1997; 94:6148-52; PMID:9177185; <http://dx.doi.org/10.1073/pnas.94.12.6148>
- Kilty I, Logan A, Vickers PJ. Differential characteristics of human 15-lipoxygenase isozymes and a novel splice variant of 15S-lipoxygenase. *Eur J Biochem* 1999; 266:83-93; PMID:10542053; <http://dx.doi.org/10.1046/j.1432-1327.1999.00818.x>
- Jisaka M, Kim RB, Boeglin WE, Nanney LB, Brash AR. Molecular cloning and functional expression of a phorbol ester-inducible 8S-lipoxygenase from mouse skin. *J Biol Chem* 1997; 272:24410-6; PMID:9305900; <http://dx.doi.org/10.1074/jbc.272.39.24410>
- Jisaka M, Kim RB, Boeglin WE, Brash AR. Identification of amino acid determinants of the positional specificity of mouse 8S-lipoxygenase and human 15S-lipoxygenase-2. *J Biol Chem* 2000; 275:1287-93; PMID:10625675; <http://dx.doi.org/10.1074/jbc.275.2.1287>
- Shappell SB, Olson SJ, Hannah SE, Manning S, Roberts RL, Masumori N, Jisaka M, Boeglin WE, Vader V, Dave DS, et al. Elevated expression of 12/15-lipoxygenase and cyclooxygenase-2 in a transgenic mouse model of prostate carcinoma. *Cancer Res* 2003; 63:2256-67; PMID:12727848
- Shureiqi I, Lippman SM. Lipoxygenase modulation to reverse carcinogenesis. *Cancer Res* 2001; 61:6307-12; PMID:11522616
- Tang S, Bhatia B, Maldonado CJ, Yang P, Newman RA, Liu J, Chandra D, Traag J, Klein RD, Fischer SM, et al. Evidence that arachidonate 15-lipoxygenase 2 is a negative cell cycle regulator in normal prostate epithelial cells. *J Biol Chem* 2002; 277:16189-201; PMID:11839751; <http://dx.doi.org/10.1074/jbc.M111936200>
- Bhatia B, Maldonado CJ, Tang S, Chandra D, Klein RD, Chopra D, Shappell SB, Yang P, Newman RA, Tang DG. Subcellular localization and tumor-suppressive functions of 15-lipoxygenase 2 (15-LOX2) and its splice variants. *J Biol Chem* 2003; 278:25091-100; PMID:12704195; <http://dx.doi.org/10.1074/jbc.M301920200>
- Tang DG, Bhatia B, Tang S, Schneider-Brossard R. 15-lipoxygenase 2 (15-LOX2) is a functional tumor suppressor that regulates human prostate epithelial cell differentiation, senescence, and growth (size). *Prostaglandins Other Lipid Mediat* 2007; 82:135-46; PMID:17164141; <http://dx.doi.org/10.1016/j.prostaglandins.2006.05.022>
- Tang S, Bhatia B, Zhou J, Maldonado CJ, Chandra D, Kim E, Fischer SM, Butler AP, Friedman SL, Tang DG. Evidence that Sp1 positively and Sp3 negatively regulate and androgen does not directly regulate functional tumor suppressor 15-lipoxygenase 2 (15-LOX2) gene expression in normal human prostate epithelial cells. *Oncogene* 2004; 23:6942-53; PMID:15247906; <http://dx.doi.org/10.1038/sj.onc.1207913>
- Bhatia B, Tang S, Yang P, Doll A, Aumüller G, Newman RA, Tang DG. Cell-autonomous induction of functional tumor suppressor 15-lipoxygenase 2 (15-LOX2) contributes to replicative senescence of human prostate progenitor cells. *Oncogene* 2005; 24:3583-95; PMID:15750631; <http://dx.doi.org/10.1038/sj.onc.1208406>
- Bhatia B, Jiang M, Suraneni M, Patrawala L, Badeaux M, Schneider-Brossard R, Multani AS, Jeter CR, Calhoun-Davis T, Hu L, et al. Critical and distinct roles of p16 and telomerase in regulating the proliferative life span of normal human prostate epithelial progenitor cells. *J Biol Chem* 2008; 283:27957-72; PMID:18662989; <http://dx.doi.org/10.1074/jbc.M803467200>
- Bhatia B, Multani AS, Patrawala L, Chen X, Calhoun-Davis T, Zhou J, Schroeder L, Schneider-Brossard R, Shen J, Pathak S, et al. Evidence that senescent human prostate epithelial cells enhance tumorigenicity: cell fusion as a potential mechanism and inhibition by p16INK4a and hTERT. *Int J Cancer* 2008; 122:1483-95; PMID:18059027; <http://dx.doi.org/10.1002/ijc.23222>
- Tang DG, Patrawala L, Calhoun T, Bhatia B, Choy G, Schneider-Brossard R, Jeter C. Prostate cancer stem/progenitor cells: identification, characterization, and implications. *Mol Carcinog* 2007; 46:1-14; PMID:16921491; <http://dx.doi.org/10.1002/mc.20255>
- Jack GS, Brash AR, Olson SJ, Manning S, Coffey CS, Smith JA Jr, Shappell SB. Reduced 15-lipoxygenase-2 immunostaining in prostate adenocarcinoma: correlation with grade and expression in high-grade prostatic intraepithelial neoplasia. *Hum Pathol* 2000; 31:1146-54; PMID:11014584; <http://dx.doi.org/10.1053/hupa.2000.16670>
- Shappell SB, Boeglin WE, Olson SJ, Kasper S, Brash AR. 15-lipoxygenase-2 (15-LOX-2) is expressed in benign prostatic epithelium and reduced in prostate adenocarcinoma. *Am J Pathol* 1999; 155:235-45; PMID:10393855; [http://dx.doi.org/10.1016/S0002-9440\(10\)65117-6](http://dx.doi.org/10.1016/S0002-9440(10)65117-6)
- Zhang J, Thomas TZ, Kasper S, Matusik RJ. A small composite probasin promoter confers high levels of prostate-specific gene expression through regulation by androgens and glucocorticoids in vitro and in vivo. *Endocrinology* 2000; 141:4698-710; PMID:11108285
- Suraneni MV, Schneider-Brossard R, Moore JR, Davis TC, Maldonado CJ, Li H, Newman RA, Kusewitt D, Hu J, Yang P, et al. Transgenic expression of 15-lipoxygenase 2 (15-LOX2) in mouse prostate leads to hyperplasia and cell senescence. *Oncogene* 2010; 29:4261-75; PMID:20514017; <http://dx.doi.org/10.1038/onc.2010.197>
- Chano T, Saji M, Inoue H, Minami K, Kobayashi T, Hino O, Okabe H. Neuromuscular abundance of RB1CC1 contributes to the non-proliferating enlarged cell phenotype through both RB1 maintenance and TSC1 degradation. *Int J Mol Med* 2006; 18:425-32; PMID:16865226
- Chano T, Ikebuchi K, Ochi Y, Tameno H, Tomita Y, Jin Y, Inaji H, Ishitobi M, Teramoto K, Nishimura I, et al. RB1CC1 activates RB1 pathway and inhibits proliferation and clonogenic survival in human cancer. *PLoS One* 2010; 5:e11404; PMID:20614030; <http://dx.doi.org/10.1371/journal.pone.0011404>
- Gan B, Guan JL. FIP200, a key signaling node to coordinately regulate various cellular processes. *Cell Signal* 2008; 20:787-94; PMID:18036779; <http://dx.doi.org/10.1016/j.cellsig.2007.10.021>
- Kontani K, Chano T, Ozaki Y, Tezuka N, Sawai S, Fujino S, Saeki Y, Okabe H. RB1CC1 suppresses cell cycle progression through RB1 expression in human neoplastic cells. *Int J Mol Med* 2003; 12:767-9; PMID:14533007
- Ellwood-Yen K, Graeber TG, Wongvipat J, Iruela-Arispe ML, Zhang J, Matusik R, Thomas GV, Sawyers CL. Myc-driven murine prostate cancer shares molecular features with human prostate tumors. *Cancer Cell* 2003; 4:223-38; PMID:14522256; [http://dx.doi.org/10.1016/S1535-6108\(03\)00197-1](http://dx.doi.org/10.1016/S1535-6108(03)00197-1)
- Gurel B, Iwata T, Koh CM, Jenkins RB, Lan F, Van Dang C, Hicks JL, Morgan J, Cornish TC, Sutcliffe S, et al. Nuclear MYC protein overexpression is an early alteration in human prostate carcinogenesis. *Mod Pathol* 2008; 21:1156-67; PMID:18567993; <http://dx.doi.org/10.1038/modpathol.2008.111>
- Gil J, Kerai P, Leonard M, Bernard D, Cigudosa JC, Peters G, Carnero A, Beach D. Immortalization of primary human prostate epithelial cells by c-Myc. *Cancer Res* 2005; 65:2179-85; PMID:15781629; <http://dx.doi.org/10.1158/0008-5472.CAN-03-4030>
- Pelengaris S, Littlewood T, Khan M, Elia G, Evan G. Reversible activation of c-Myc in skin: induction of a complex neoplastic phenotype by a single oncogenic lesion. *Mol Cell* 1999; 3:565-77; PMID:10360173; [http://dx.doi.org/10.1016/S1097-2765\(00\)80350-0](http://dx.doi.org/10.1016/S1097-2765(00)80350-0)
- Pelengaris S, Khan M, Evan G. c-MYC: more than just a matter of life and death. *Nat Rev Cancer* 2002; 2:764-76; PMID:12360279; <http://dx.doi.org/10.1038/nrc904>
- Pelengaris S, Khan M, Evan GI. Suppression of Myc-induced apoptosis in beta cells exposes multiple oncogenic properties of Myc and triggers carcinogenic progression. *Cell* 2002; 109:321-34; PMID:12015982; [http://dx.doi.org/10.1016/S0092-8674\(02\)00738-9](http://dx.doi.org/10.1016/S0092-8674(02)00738-9)
- Chen Z, Trotman LC, Shaffer D, Lin HK, Dotan ZA, Niki M, Koutcher JA, Scher HI, Ludwig T, Gerald W, et al. Crucial role of p53-dependent cellular senescence in suppression of Pten-deficient tumorigenesis. *Nature* 2005; 436:725-30; PMID:16079851; <http://dx.doi.org/10.1038/nature03918>
- Shappell SB, Thomas GV, Roberts RL, Herbert R, Ittmann MM, Rubin MA, Humphrey PA, Sundberg JP, Rozengurt N, Barrios R, et al. Prostate pathology of genetically engineered mice: definitions and classification. The consensus report from the Bar Harbor meeting of the Mouse Models of Human Cancer Consortium Prostate Pathology Committee. *Cancer Res* 2004; 64:2270-305; PMID:15026373; <http://dx.doi.org/10.1158/0008-5472.CAN-03-0946>

31. Liu P, Ramachandran S, Ali Seyed M, Scharer CD, Laycock N, Dalton WB, Williams H, Karanam S, Datta MW, Jaye DL, et al. Sex-determining region Y box 4 is a transforming oncogene in human prostate cancer cells. *Cancer Res* 2006; 66:4011-9; PMID:16618720; <http://dx.doi.org/10.1158/0008-5472.CAN-05-3055>
32. Taylor BS, Schultz N, Hieronymus H, Gopalan A, Xiao Y, Carver BS, Arora VK, Kaushik P, Cerami E, Reva B, et al. Integrative genomic profiling of human prostate cancer. *Cancer Cell* 2010; 18:11-22; PMID:20579941; <http://dx.doi.org/10.1016/j.ccr.2010.05.026>
33. Abate-Shen C, Banach-Petrosky WA, Sun X, Economides KD, Desai N, Gregg JP, Borowsky AD, Cardiff RD, Shen MM. Nkx3.1; Pten mutant mice develop invasive prostate adenocarcinoma and lymph node metastases. *Cancer Res* 2003; 63:3886-90; PMID:12873978
34. Kim MJ, Cardiff RD, Desai N, Banach-Petrosky WA, Parsons R, Shen MM, Abate-Shen C. Cooperativity of Nkx3.1 and Pten loss of function in a mouse model of prostate carcinogenesis. *Proc Natl Acad Sci U S A* 2002; 99:2884-9; PMID:11854455; <http://dx.doi.org/10.1073/pnas.042688999>
35. Chano T, Ikegawa S, Kontani K, Okabe H, Baldini N, Saeki Y. Identification of RB1CC1, a novel human gene that can induce RB1 in various human cells. *Oncogene* 2002; 21:1295-8; PMID:11850849; <http://dx.doi.org/10.1038/sj.onc.1205178>
36. Mahipal SV, Subhashini J, Reddy MC, Reddy MM, Anilkumar K, Roy KR, Reddy GV, Reddanna P. Effect of 15-lipoxygenase metabolites, 15-(S)-HPETE and 15-(S)-HETE on chronic myelogenous leukemia cell line K-562: reactive oxygen species (ROS) mediate caspase-dependent apoptosis. *Biochem Pharmacol* 2007; 74:202-14; PMID:17517376; <http://dx.doi.org/10.1016/j.bcp.2007.04.005>
37. Rao GN, Glasgow WC, Eling TE, Runge MS. Role of hydroperoxyeicosatetraenoic acids in oxidative stress-induced activating protein 1 (AP-1) activity. *J Biol Chem* 1996; 271:27760-4; PMID:8910370; <http://dx.doi.org/10.1074/jbc.271.44.27760>
38. Tomlins SA, Mehra R, Rhodes DR, Cao X, Wang L, Dhanasekaran SM, Kalyana-Sundaram S, Wei JT, Rubin MA, Pienta KJ, et al. Integrative molecular concept modeling of prostate cancer progression. *Nat Genet* 2007; 39:41-51; PMID:17173048; <http://dx.doi.org/10.1038/ng1935>
39. Chano T, Kontani K, Teramoto K, Okabe H, Ikegawa S. Truncating mutations of RB1CC1 in human breast cancer. *Nat Genet* 2002; 31:285-8; PMID:12068296; <http://dx.doi.org/10.1038/ng911>
40. Tang Y, Wang MT, Chen Y, Yang D, Che M, Honn KV, Akers GD, Johnson SR, Nie D. Downregulation of vascular endothelial growth factor and induction of tumor dormancy by 15-lipoxygenase-2 in prostate cancer. *Int J Cancer* 2009; 124:1545-51; PMID:19089921; <http://dx.doi.org/10.1002/ijc.24118>
41. Ikebuchi K, Chano T, Ochi Y, Tameno H, Shimada T, Hisa Y, Okabe H. RB1CC1 activates the promoter and expression of RB1 in human cancer. *Int J Cancer* 2009; 125:861-7; PMID:19437535; <http://dx.doi.org/10.1002/ijc.24466>
42. Ochi Y, Chano T, Ikebuchi K, Inoue H, Isono T, Arai A, Tameno H, Shimada T, Hisa Y, Okabe H. RB1CC1 activates the p16 promoter through the interaction with hSNF5. *Oncol Rep* 2011; 26:805-12; PMID:21637919
43. Thomasson M, Wang B, Hammarsten P, Dahlman A, Persson JL, Josefsson A, Stattin P, Granfors T, Egevad L, Henriksson R, et al. LRIG1 and the liar paradox in prostate cancer: a study of the expression and clinical significance of LRIG1 in prostate cancer. *Int J Cancer* 2011; 128:2843-52; PMID:21128282; <http://dx.doi.org/10.1002/ijc.25820>
44. Badeaux MA, Jeter CR, Gong S, Liu B, Suraneni MV, Rundhaug J, Fischer SM, Yang T, Kusewitt D, Tang DG. In vivo functional studies of tumor-specific retrogene NanogP8 in transgenic animals. *Cell Cycle* 2013; 12:2395-408; PMID:23839044; <http://dx.doi.org/10.4161/cc.25402>
45. Gundersen HJ, Bagger P, Bendtsen TF, Evans SM, Korbo L, Marcussen N, Møller A, Nielsen K, Nyengaard JR, Pakkenberg B, et al. The new stereological tools: disector, fractionator, nucleator and point sampled intercepts and their use in pathological research and diagnosis. *APMIS* 1988; 96:857-81; PMID:3056461; <http://dx.doi.org/10.1111/j.1699-0463.1988.tb00954.x>
46. López-Beltrán A, Artacho-Pérula E, Luque-Barona RJ, Roldán-Villalobos R. Nuclear volume estimates in prostatic atypical adenomatous hyperplasia. *Anal Quant Cytol Histol* 2000; 22:438-44; PMID:11147297
47. Liu C, Kelnar K, Liu B, Chen X, Calhoun-Davis T, Li H, Patrawala L, Yan H, Jeter C, Honorio S, et al. The microRNA miR-34a inhibits prostate cancer stem cells and metastasis by directly repressing CD44. *Nat Med* 2011; 17:211-5; PMID:21240262; <http://dx.doi.org/10.1038/nm.2284>